CHEMISTRY OF MATERIALS
Article

Chem. Mater. **2009,** *21,* 4261–4274 4261
DOI:10.1021/cm901430t

Surface Electroinitiated Emulsion Polymerization (SEEP): A Mechanistic Approach

Lorraine Tessier,[†] Guy Deniau,*[,†] Bernadette Charleux,[‡] and Serge Palacin[†]

[†]*CEA-Saclay, DSM-IRAMIS-SPCSI, F-91191 Gif-sur-Yvette Cedex, France, and* [‡]*UPMC and CNRS, Université Paris 6, UMR 7610, Laboratoire de Chimie des Polymères, 4 Place Jussieu, Tour 44, couloir 44-54, 1er étage, 75252 Paris Cedex 05, France*

Received May 26, 2009. Revised Manuscript Received July 21, 2009

As recently reported, the SEEP process (surface electroinitiated emulsion polymerization) is a new grafting method that provides covalently grafted polymer films on conducting or semiconducting surfaces by radical polymerization in aqueous dispersed media. It relies on cathodic electroinitiation, which creates radical species able to start a radical polymerization. Contrary to the formerly described cathodic electrografting of vinylic polymers (CE), which also delivers submicrometer-thick and stable polymer films on conducting substrates but requires strictly anhydrous conditions and organic aprotic solvent, SEEP brings a major improvement in switching from a purely anionic mechanism to a radical one by adding an aryldiazonium salt in the reaction mixture, while retaining the same polymer films characteristics. Moreover, SEEP is not restricted to water-soluble monomers but can be performed even with hydrophobic ones, such as *n*-butyl methacrylate (BMA). In such cases, a surfactant is necessary to stabilize the monomer in water emulsion. From this one-pot electrografting process performed in water at room temperature, in a few minutes, without restrictions on vinylic monomer water solubility, results a polymer coating strongly grafted to the substrate. This article aims at completing our first one and focuses on mechanistic aspects of SEEP to eventually establish a possible "grafting onto" mechanism. To achieve that goal, we have analyzed grafted polymer films obtained by SEEP on gold substrate from BMA in water as a miniemulsion by IR-ATR, X-ray photoelectron spectroscopy (XPS), time-of-flight secondary ion mass spectroscopy (ToF-SIMS), and atomic force microscopy (AFM).

1. Introduction

If we consider that materials properties are often directly expressed by their surface, organic coatings and more particularly polymer thin films are nowadays a very attractive research subject related to many and various fields of application such as depollution, microelectronics, automobile, biomedical tools engineering, lubrication, etc. Indeed, surface modification by resistant polymer coatings confer on materials many properties (antifouling, antisoiling, adhesion, lubrication, biocompatibilization) targeted by those industries. In consequence, a large range of coating methods, including "physisorption" or "chemisorption" techniques, has been investigated to synthesize organic or composite layers. Physisorption techniques such as painting, spin coating, and vacuum evaporation, have no limitation for choosing the substrate−layer couple, but the weak interactions involved at the interfacial zone result in fragility of the coating and possible loss of the desired properties with time. On the contrary, "chemisorption" techniques, including plasma polymerization,[1,2] self-assembly,[3,4] and in situ surface polymerizations, seem by far the most convenient to get stable films. Among them, the latter appears to be a method of choice for a strong covalent attachment of polymer chains as ultrathin films to the surface. Among in situ surface polymerizations, it is important to distinguish "grafting to" from "grafting from" ways. The first one involves the bonding of preformed end-functionalized polymer chains to the surface, and the second one, also called surface-initiated polymerization,[5−7] means that the polymer growth (initiation and propagation) occurs from the surface. From this, it is possible to adapt any classical bulk polymerization to form grafted polymer brushes by modifying the substrate with initiator-bearing monolayer in a first step.[8−14] Obviously, living polymerizations such as controlled radical polymerizations (CRP) are well suited to

*Corresponding author. Tel.: 33 1 69 08 21 11. Fax: 33 1 69 08 64 62. E-mail: guy.deniau@cea.fr.

(1) Bodas, D. S.; Desai, S. M.; Gangal, S. A. *Appl. Surf. Sci.* **2005**, *245*, 186–190.
(2) Pan, Q.; Wang, M.; Chen, W. *Chem. Lett.* **2007**, *36*, 1312–1313.
(3) Love, J. C.; Estroff, L. A.; Kriebel, J. K.; Nuzzo, R. G.; Whitesides, G. M. *Chem. Rev.* **2005**, *105*, 1103–1170.
(4) Heister, K.; Zharnikov, M.; Grunze, M.; Johansson, L. S. O.; Ulman, A. *Langmuir* **2001**, *17*, 8–11.
(5) Edmondson, S.; Osborne, V, L.; Huck, W. T. S. *Chem. Soc. Rev.* **2004**, *33*, 14–22.
(6) *Surface-Initiated Polymerization I*; Jordan, R. Ed.; Advances in Polymer Science; Springer-Verlag: Berlin, 2006; Vol. *197*.
(7) Adenier, A.; Cabet-Deliry, E.; Lalot, T.; Pinson, J.; Podvorica, F. *Chem. Mater.* **2002**, *14*, 4576–4585.
(8) Prucker, O.; Rühe, J. *Macromolecules* **1998**, *31*, 592–601.
(9) Prucker, O.; Rühe, J. *Langmuir* **1998**, *14*, 6893–6898.
(10) Advincula, R. In *Surface-Initiated Polymerization I*; Jordan, R. Ed.; Advances in Polymer Science; Springer-Verlag, Berlin, 2006; Vol. *197*, p 107−136.

Published on Web 08/24/2009

achieve maximum control over brush density, chain polydispersity, composition, molecular weight, and thickness of the grafted polymer brushes.[15−18] Especially surface-initiated ATRP (SI ATRP)[5,16,17] have become the most popular route, mostly because of its tolerance to a wide range of functional monomers and its possibility to form block copolymers and several architectures.[19] Surface-initiated polymerization and more particularly SI ATRP proceeds in two steps: (i) immobilization of the initiators by suitable surface chemistry; (ii) polymerization in classical ATRP conditions. Yet, the presence of copper in the second step performed at high temperature makes industrial applications difficult.

In parallel, electrochemical reduction of diazonium salts has been widely investigated for the past ten years and become almost ubiquitous for easy surface modification.[20] It is a simple and versatile way to graft thin organic layers onto carbon[21−25] and carbon nanotubes,[26−28] noble[29,30] or industrial metals,[31−34] and semiconductors (Si,[35−38] ITO,[39] and diamond[40−42]). The mechanism involves aryl radicals, resulting from the electroreduction of diazonium precursors concerted with the cleavage of dinitrogen. Aryl radicals thus formed are covalently bonded to the substrate via carbon−metal bonds.[43] Furthermore, aryl radicals formed in excess may react with already grafted aryl groups to form aryl-to-aryl links.[25,29,36,44,45] That method delivers only very thin polyaryl coatings, but was already used with halogenated (brominated) aryldiazonium salts[46] that eventually act as initiators in ATRP. Therefore, by choosing the appropriate diazonium salt, "diazonium-based" ATRP can be performed with many monomers (styrene, methylmethacrylate, butylmethacrylate) from several substrates.[46−50]

Unlike the previous processes, cathodic electrografting of activated vinylic monomers (CE)[51] is a one-electrochemical-step process that relies on a direct electroinitiation of the monomer, reduced under a cathodic current, in a very unstable radical-anion immobilized on the electrode. Then, the chain growth proceeds from the surface by purely anionic propagation. The reaction mechanism of electrografting was in particular described by Bureau et al.[52] and the covalent carbon-to-metal bond was evidenced using XPS.[53] In spite of significant advantages to produce thick and resilient organic coatings truly grafted onto any conducting substrates, CE suffers from several drawbacks that obviously limit its practical use. The main disadvantage is its anionic mechanism, which requires strictly anhydrous conditions: use of aprotic organic solvents and a limited choice of vinylic monomers restricted to (meth)acrylic derivatives.[54] CE and

(11) Fulghum, T. M.; Taranekar, P.; Advincula, R. C. *Macromolecules* **2008**, *41*, 5681–5687.
(12) Bialk, M.; Prucker, O.; Rühe, J. *Colloid Surf., A* **2002**, *198*, 543–549.
(13) Raghuraman, G. K.; Dhamodharan, R.; Prucker, O.; Rühe, J. *Macromolecules* **2008**, *41*, 873–878.
(14) Schuh, K.; Prucker, O.; Rühe, J. r. *Macromolecules* **2008**, *41*, 9284–9289.
(15) Husseman, M.; Malmstrom, E. E.; McNamara, M.; Mate, M.; Mecerreyes, D.; Benoit, D. G.; Hedrick, J. L.; Mansky, P.; Huang, E.; Russell, T. P.; Hawker, C. J. *Macromolecules* **1999**, *32*, 1424–1431.
(16) Kato, M.; Kamigaito, M.; Sawamoto, M.; Higashimura, T. *Macromolecules* **1995**, *28*, 1721–1723.
(17) Wang, J.-S.; Matyjaszewski, K. *J. Am. Chem. Soc.* **1995**, *117*, 5614–5615.
(18) Baum, M.; Brittain, W. J. *Macromolecules* **2002**, *35*, 610–615.
(19) Matyjaszewski, K.; Qin, S.; Boyce, J. R.; Shirvanyants, D.; Sheiko, S. S. *Macromolecules* **2003**, *36*, 1843–1849.
(20) Pinson, J.; Podvorica, F. *Chem. Soc. Rev.* **2005**, *34*, 429–439.
(21) Allongue, P.; Delamar, M.; Desbat, B.; Fagebaume, O.; Hitmi, R.; Pinson, J.; Saveant, J. M. *J. Am. Chem. Soc.* **1997**, *119*, 201–207.
(22) Delamar, M.; Hitmi, R.; Pinson, J.; Saveant, J. M. *J. Am. Chem. Soc.* **1992**, *114*, 5883–5884.
(23) Liu, Y.-C.; McCreery, R. L. *J. Am. Chem. Soc.* **1995**, *117*, 11254–11259.
(24) Ortiz, B.; Saby, C.; Champagne, G. Y.; Bélanger, D. *J. Electroanal. Chem.* **1998**, *455*, 75–81.
(25) Anariba, F.; DuVall, S. H.; McCreery, R. L. *Anal. Chem.* **2003**, *75*, 3837–3844.
(26) Bahr, J. L.; Yang, J.; Kosynkin, D. V.; Bronikowski, M. J.; Smalley, R. E.; Tour, J. M. *J. Am. Chem. Soc.* **2001**, *123*, 6536–6542.
(27) Dyke, C. A.; Tour, J. M. *Nano Lett.* **2003**, *3*, 1215–1218.
(28) Schmidt, G.; Gallon, S.; Esnouf, S.; Bourgoin, J.-P.; Chenevier, P. *Chem.—Eur. J.* **2009**, *15*, 2101–2110.
(29) Bernard, M.-C.; Chausse, A.; Cabet-Deliry, E.; Chehimi, M. M.; Pinson, J.; Podvorica, F.; Vautrin-Ul, C. *Chem. Mater.* **2003**, *15*, 3450–3462.
(30) Laforgue, A.; Addou, T.; Bélanger, D. *Langmuir* **2005**, *21*, 6855–6865.
(31) Hurley, B. L.; McCreery, R. L. *J. Electrochem. Soc.* **2004**, *151*, B252–B259.
(32) Adenier, A.; Bernard, M. C.; Chehimi, M. M.; Cabet-Deliry, E.; Desbat, B.; Fagebaume, O.; Pinson, J.; Podvorica, F. *J. Am. Chem. Soc.* **2001**, *123*, 4541–4549.
(33) Chausse, A.; Chehimi, M. M.; Karsi, N.; Pinson, J.; Podvorica, F.; Vautrin-Ul, C. *Chem. Mater.* **2002**, *14*, 392–400.
(34) Adenier, A.; Cabet-Deliry, E.; Chaussé, A.; Griveau, S.; Mercier, F.; Pinson, J.; Vautrin-Ul, C. *Chem. Mater.* **2005**, *17*, 491–501.
(35) Allongue, P.; Henry de Villeneuve, C.; Pinson, J.; Ozanam, F.; Chazalviel, J. N.; Wallart, X. *Electrochim. Acta* **1998**, *43*, 2791–2798.
(36) Allongue, P.; Henry de Villeneuve, C.; Cherouvrier, G.; Cortès, R.; Bernard, M. C. *J. Electroanal. Chem.* **2003**, *550−551*, 161–174.
(37) Henry de Villeneuve, C.; Pinson, J.; Bernard, M. C.; Allongue, P. *J. Phys. Chem. B* **1997**, *101*, 2415–2420.
(38) Stewart, M. P.; Maya, F.; Kosynkin, D. V.; Dirk, S. M.; Stapleton, J. J.; McGuiness, C. L.; Allara, D. L.; Tour, J. M. *J. Am. Chem. Soc.* **2004**, *126*, 370–378.
(39) Maldonado, S.; Smith, T. J.; Williams, R. D.; Morin, S.; Barton, E.; Stevenson, K. J. *Langmuir* **2006**, *22*, 2884–2891.
(40) Lud, S. Q.; Steenackers, M.; Jordan, R.; Bruno, P.; Gruen, D. M.; Feulner, P.; Garrido, J. A.; Stutzmann, M. *J. Am. Chem. Soc.* **2006**, *128*, 16884–16891.
(41) Uetsuka, H.; Shin, D.; Tokuda, N.; Saeki, K.; Nebel, C. E. *Langmuir* **2007**, *23*, 3466–3472.
(42) Wang, J.; Firestone, M. A.; Auciello, O.; Carlisle, J. A. *Langmuir* **2004**, *20*, 11450–11456.
(43) Boukerma, K.; Chehimi, M. M.; Pinson, J.; Blomfield, C. *Langmuir* **2003**, *19*, 6333–6335.
(44) Kariuki, J. K.; McDermott, M. T. *Langmuir* **1999**, *15*, 6534–6540.
(45) Kariuki, J. K.; McDermott, M. T. *Langmuir* **2001**, *17*, 5947–5951.
(46) Matrab, T.; Chehimi, M. M.; Perruchot, C.; Adenier, A.; Guillez, A.; Save, M.; Charleux, B.; Cabet-Deliry, E.; Pinson, J. *Langmuir* **2005**, *21*, 4686–4694.
(47) Matrab, T.; Chehimi, M. M.; Boudou, J. P.; Benedic, F.; Wang, J.; Naguib, N. N.; Carlisle, J. A. *Diamond Relat. Mater.* **2006**, *15*, 639–644.
(48) Matrab, T.; Chehimi, M. M.; Pinson, J.; Slomkowski, S.; Basinska, T. *Surf. Interface Anal.* **2006**, *38*, 565–568.
(49) Matrab, T.; Save, M.; Charleux, B.; Pinson, J.; Cabet-deliry, E.; Adenier, A.; Chehimi, M. M.; Delamar, M. *Surf. Sci.* **2007**, *601*, 2357–2366.
(50) Matrab, T.; Chancolon, J.; L'Hermite, M. M.; Rouzaud, J.-N.; Deniau, G.; Boudou, J.-P.; Chehimi, M. M.; Delamar, M. *Colloids Surf., A* **2006**, *287*, 217–221.
(51) Palacin, S.; Bureau, C.; Charlier, J.; Deniau, G.; Mouanda, B.; Viel, P. *ChemPhysChem* **2004**, *5*, 1468–1481.
(52) Bureau, C.; Delhalle, J. *J. Surf. Anal.* **1999**, *6*, 159–170.
(53) Deniau, G.; Azoulay, L.; Jégou, P.; Le Chevallier, G.; Palacin, S. *Surf. Sci.* **2006**, *600*, 675–684.
(54) Baute, N.; Teyssié, P; Martinot, L.; Mertens, M.; Dubois, P.; Jérôme, R. *Eur. J. Inorg. Chem.* **1998**, *1998*, 1711–1720.

SI-ATRP techniques have been recently compared[55] and although they are valuable tools for the synthesis of grafted organic coatings on conducting surfaces, both processes have drawbacks: higher monomer concentration, longer polymerization time and heating are required for the SI-ATRP process; more drastic anhydrous conditions, and a narrower choice of monomers limit the expansion of the cathodic electrografting process.

CE and SI-ATRP drawbacks would obviously be overcome with an alternative electrografting method based on a radical mechanism. Recently, aryldiazonium salts have been shown to be good initiators[56,57] in radical polymerization. Thus, by applying a cathodic current to a mixture containing both a diazonium salt and a vinylic monomer, polymer chains are actually found grafted on the cathode. This led to a new powerful process called SEEP for surface electroinitiated emulsion polymerization. SEEP provides various organic coatings strongly grafted on conducting or semiconducting substrates[58] and may be seen as a very significant improvement from CE and SI-ATRP. The key point of that improvement versus CE is to switch from a direct anionic way to a radical one thanks to outstanding properties of diazonium salts. In that case, electrografting is accessible to a wide range of monomers and can be performed in aqueous media, homogeneous or heterogeneous, according to the monomer water solubility. Regarding the film structure, as SEEP includes aryldiazonium salts, the resulting polymer films are actually polyaryl−polyvinylic copolymers.

Most importantly, as already described in our previous article introducing this new technique, SEEP is a one-pot process (unlike SI-ATRP) that works in aqueous dispersed media from available reagents without any catalyst and with low reaction times, which makes it perfectly acceptable from an industrial point of view. The only described competing method relies on very specific synthesized amphiphilic monomers that play the role of surfactant, initiator, and monomer at the same time.[59]

Our previous paper[58] gave a preliminary description of this process. Various monomers of different water solubility were reviewed proving the versatility of the process. Moreover, a brief discussion on a tentative mechanism had been proposed.

The present work aims at completing and reinforcing that first SEEP article from the mechanistic aspects. Our objective here is to bring new information about film morphology, molecular structure, and initiating species in order to highlight some unclear mechanistic points. In a first part, we will describe SEEP through new characterizations. Then, a fine molecular structure of the coating will be determined insisting on the ubiquity of nitrophenyl groups originating from the diazonium initiator. In a third part, emphasis will be placed on the proton reduction and the initiation of the polymerization process by hydrogen radical will be evidenced. Finally, a complete build-up mechanism will be detailed specifying where the polymerization reaction takes place in the biphasic medium.

For clarity reasons, the study is almost entirely restricted to *n*-butyl methacrylate as a monomer and to flat gold substrates even if SEEP proved to be efficient on various electrode geometries, including "pseudo-3D" electrodes such as carbon nanotubes carpets that were found homogeneously coated by the selected vinylic polymer.[60] BMA was chosen as a model monomer because of its low solubility in water and its ability to undergo radical emulsion polymerization.

2. Experimental Section

2.1. Mixture Preparation. *n*-Butyl methacrylate (BMA, Aldrich, 99%) and hydroxyethyl methacrylate (HEMA, Aldrich, 99%) were distilled under reduce pressure before use to remove the inhibitors and stored at low temperature. Sodium dodecyl sulfate (SDS, Aldrich, 98.5%) and 4-nitrobenzene diazonium (NBD) tetrafluoroborate (Aldrich, 97%) were purchased from Aldrich and used as received.

A master acidic solution at 1×10^{-2} M (pH $\leq$ 2) was prepared from pure sulfuric acid (VWR, 95%) in deionized water (DI water).

For grafting of poly(*n*-butyl methacrylate) (PBMA), a heterogeneous mixture was prepared due to the limited water-solubility of BMA (2.5×10^{-3} M). Miniemulsions were obtained by adding in 50 mL of the master acidic solution, SDS (0.13 g, 9×10^{-3} M = 1.125 CMC (Critical Micelle Concentration of SDS[61] is $8.2.10^{-3}$ M)) and the insoluble BMA monomer (4.98 g, 0.7 M). The turbid water/oil mixture was then submitted to ultrasonication (ultrasonic processor; power 60% × 130 W) for 10 min. Then NBD (0.0237 g, 2×10^{-3} M) was added under magnetic stirring. The resulting reacting medium was actually a complex heterogeneous mixture at a microscopic scale, containing many compounds organized as shown in Scheme 1. Contrary to our first paper,[58] the biphasic monomer-in-water system was strongly sheared by ultrasonication similarly to a miniemulsion,[62] in order to form small monomer droplets and enhance stability. No hydrophobe such as *n*-hexadecane typically used to avoid Ostwald ripening was however added. In these conditions, the miniemulsion stability was reduced with respect to that observed in the presence of the hydrophobe and a biphasic system was recovered in a few hours (4−5 h). Such procedure was applied because it led to the best grafting results.

2.2. Preparation of Gold Substrates. Gold substrates were obtained by vacuum evaporation of pure gold (99.99% from Williams Advanced Materials) at room temperature on 76 × 13 mm^2 glass plates supplied by RS France. In a Balzers BAK 600 evaporator, a 2−10 nm chromium underlayer was first deposited to enhance gold adhesion on glass and then 40 − 200 nm of gold was evaporated under a residual pressure of 1×10^{-7} bar, at room temperature, at an evaporation speed of 5 nm min^{-1}. Gold plates were used without further cleaning treatment.

(55) Mouanda, B.; Bassa, E.; Deniau, G.; Jegou, P.; Viel, P.; Palacin, S. *J. Electroanal. Chem.* **2009**, *629*, 102–109.
(56) Markus, R. H. *Chem.—Eur. J.* **2009**, *15*, 820–833.
(57) Zhang, X.; Bell, J. P. *J. Appl. Polym. Sci.* **1999**, *73*, 2265–2272.
(58) Deniau, G.; Azoulay, L.; Bougerolles, L.; Palacin, S. *Chem. Mater.* **2006**, *18*, 5421–5428.
(59) Cécius, M.; Jérôme, R.; Jérôme, C. *Macromol. Rapid Commun.* **2007**, *28*, 948–954.
(60) Tessier, L.; Chancolon, J.; Alet, P.-J.; Trenggono, A.; Mayne-L'Hermite, M.; Deniau, G.; Jégou, P.; Palacin, S. *Phys. Status Solidi A* **2008**, *205*, 1412–1418.
(61) Terabe, S.; Otsuka, K.; Ichikawa, K.; Tsuchiya, A.; Ando, T. *Anal. Chem.* **1984**, *56*, 111–113.
(62) Daniel, J.-C.; Pichot, C. *Les Latex Synthétiques*; Tec & Doc Lavoisier: Paris, 2005.

Scheme 1. Composition of the Initial Miniemulsion System in the Electrochemical Cell

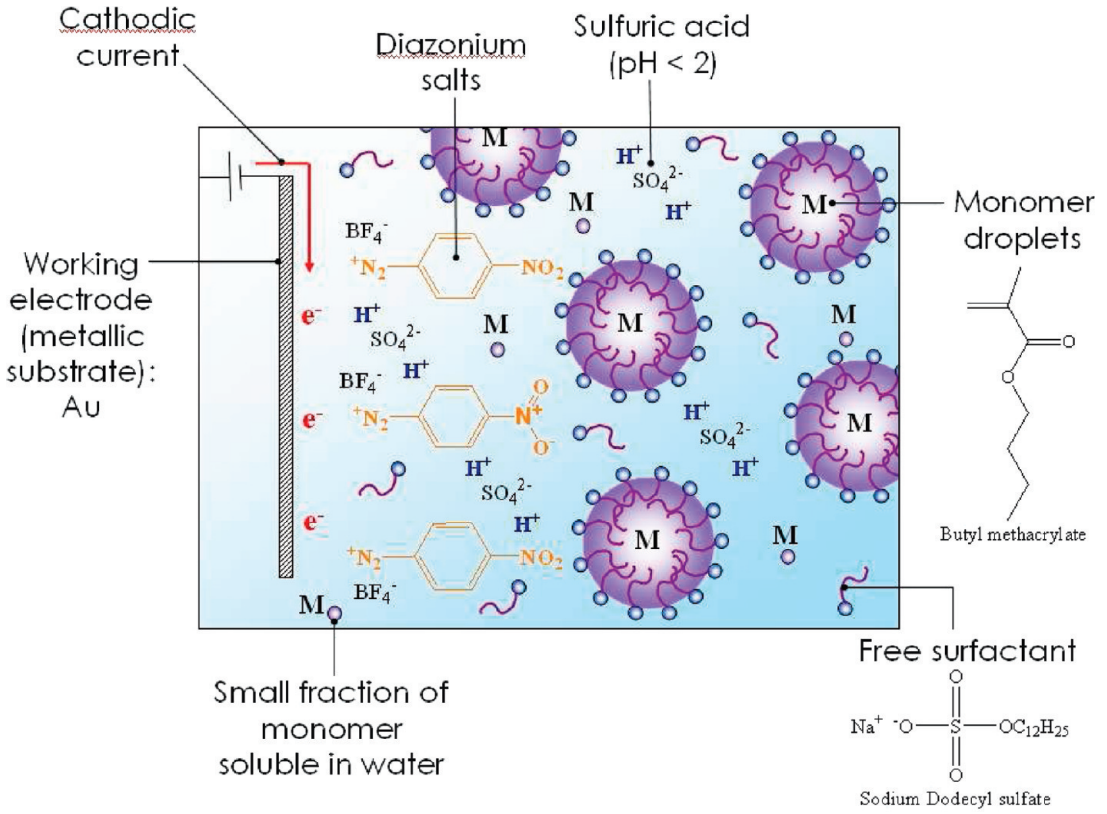

2.3. Electrochemical Procedures. Electrochemical syntheses were carried out under argon in a three-electrode cell with a Princeton Applied Research Inc. potentiostat model 263A from EG&G. The working electrode polarization was achieved under cyclic voltamperometry ranging from 1 to 10 cycles at 10 mV s^{-1} scanning rate from the rest potential (~0.5 V) to the final potential, usually at −1.0 V. A low scan rate was used in all SEEP experiments because the thickness of the grafted film was found higher than with faster scan rates in similar conditions. Working electrode was a smooth Au surface obtained as previously described, counter electrode was a graphite plate and a saturated calomel electrode (SCE) was used as the reference. Thus, in voltamperograms, potentials are given versus SCE and current values are given for roughly 2.5 cm^2 of gold surface dipped into the solution. The reaction time depends on the number of cycles (~30 min for 5 cycles). The experiments were conducted at room temperature in acidic deionized water because of the instability of the diazonium group in presence of nucleophiles such as hydroxide ions in more basic medium.[63] Miniemulsions were systematically deoxygenated by argon bubbling under stirring for 30 min before electrochemical treatments to remove dioxygen (radical polymerization inhibitor), and then a constant blanket of Ar was maintained above the miniemulsion, whereas magnetic stirring was stopped during the experiment.

After all experiments, to ensure the covalent character of the grafting, samples were systematically rinsed with DI water and acetone and, finally, dipped into dimethylformamide (DMF) under ultrasonication (40 W) for 30 s in order to both remove any physisorbed polymer chains and test the strength of the film attachment.

Electrochemical quartz crystal microbalance (EQCM) experiments were performed using a 5 mm diameter quartz crystal (9 MHz) gold metalized on both faces purchased from BIO-LOGIC and used as received. The quartz crystal was set in a holder made of Teflon and connected to a three-electrode cell especially designed to host it, composed of a graphite counter electrode, a saturated calomel reference electrode and the working electrode consisting of the gold coated quartz (area 0.2 cm^2). Electrochemical experiments were performed using an EG&G Princeton Applied Research model 283 potentiostat and a SEIKO 922 QCM model. The Δf out connector was connected to the external ADC input of the potentiostat. Three calibration sensibilities are available for the measurements of the eigenfrequency shifts.

2.4. Spectroscopic Analyses. Infrared spectra were obtained on a Bruker VERTEX 70 spectrometer equipped with ATR (Attenuated Total Reflection) Pike-Miracle device. The detector was a MCT working at liquid nitrogen temperature. The spectra were obtained after 256 scans at 2 cm^{-1} resolution.

X-ray Photoelectron Spectroscopy (XPS) analyses were performed with a Kratos Axis Ultra DLD using a high-resolution monochromatic Al Kα line X-ray source at 1486.6 eV. Fixed analyzer pass energy of 20 eV was used for core level scans. The photoelectron takeoff angle was always normal to the surface, which provides an integrated sampling depth of approximately 15 nm. A survey spectrum and core-level spectra of C1s (280−290 eV), O1s (526−538 eV) and N1s (396−410 eV) regions were systematically recorded. The energy scale of the instrument was calibrated by setting Au $4f_{7/2}$ = 84.00 eV, $Ag3d_{5/2}$ = 368.70 eV, $CuL_3M_{4,5}M_{4,5}$ = 567.90 eV and Cu $2p_{3/2}$ = 932.65 eV.[64] When charging phenomena occur, the charge is counterbalanced by

(63) Zollinger, H. *Diazo Chemistry I: Aromatic and Heteroaromatic Compounds*; VCH: Weinheim, Germany, 1994.

(64) Briggs, D.; Seah, M. P. *Practical Surface Analysis*, 2nd ed.; Wiley: New York, 1990; Vol. *1*.

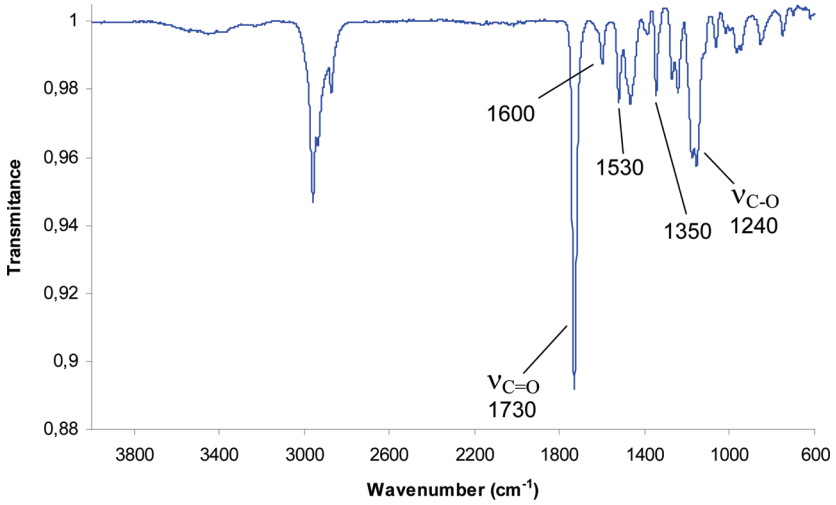

Figure 1. Typical IR-ATR spectrum of PBMA grafted by SEEP of BMA in miniemulsion (5 cycles/−1.0 V/10 mV s^{-1}) on gold substrate (wavenumber in cm^{-1} of major absorption bands; see Table 1 for the attribution).

adjusting the C1s (aliphatic carbon) level at 285 eV. However, in our case of very thin polymer films, the charge never exceeds 1−2 eV. Spectra were treated with Avantage software.

ToF-SIMS analyses were carried out with a ToF-SIMS IV ION-TOF spectrometer. Surface spectroscopic analyses were performed with Au^+ primary ions at 25 keV on a 150 × 150 μm^2 surface area in positive and negative polarity and the acquisition time was 75 s. Profiles analyses were also carried out in negative polarity using a Cs^+ gun at 500 V to dig a 500 × 500 μm^2 crater area. Acquisition times depend on the film thickness.

2.5. Atomic Force Microscopy (AFM). PBMA films were imaged by AFM in acoustic mode with a Molecular Imaging PicoSPMLe commercial AFM microscope (PicoScan 2100 controller, Scientec, France) using a commercial pyramidal Si tip (mounted on 225 μm long single-beam cantilever with a resonance frequency of approximately 75 kHz and a spring constant of about 3 N m^{-1}). The scan rate was in the range of 0.25 Hz with a scanning density of 512 lines per frame. The AFM is mounted on a floating table to achieve vibration isolation during investigations.

3. Results and Discussion

3.1. Poly(*n*-butyl methacrylate) Film Characterization. This first part gives a brief reminder of the major characteristics of SEEP, on the particular example of PBMA electrografted from a miniemulsion. Typical thin PBMA films (20−50 nm thick) were obtained from 5 voltamperometric cycles at −1.0 V. The corresponding voltamperogramm (see the Supporting Information, Figure SI-1) exhibits a reduction peak (0.25 V; 160 μA) attributed to the diazonium reduction into aryl radicals ($^{\bullet}C_6H_5-NO_2$)[22] that almost disappears after the first cycle. At lower potentials, the observed current, which remains quite significant even after several cycles, arises from the reduction of the solvent−electrolyte (DI $H_2O-H_2SO_4$), which starts at −0.4 V, leading to the reduction of protons to produce dihydrogen (H^+/H_2). That current emphasizes that the accessibility of the electrode is not totally suppressed upon the formation of the grafted film.

As shown in Figure 1, the IR-ATR spectrum of the grafted film confirms the presence of PBMA, together with nitro moieties originating from the electroreduction of the diazonium precursor (Table 1). As for previously described examples,[58] no change was observed in the IR intensity upon ultrasonication, which confirms the covalent grafting. In conclusion, this spectrum presents all the features of a poly(nitrophenylene) (PNP)−PBMA copolymer.

Table 1. Major IR Absorption Bands in a PBMA Film Synthesized by SEEP

	wavenumber (cm^{-1})							
	2958	2932	2870	1730	1600	1530	1350	1240
attribution	ν^{as}_{CH3}	ν^{as}_{CH2}	ν^{s}_{CH2}	$\nu_{C=O}$	$\nu_{C=C}$	ν^{as}_{NO2}	ν^{s}_{NO2}	ν_{OCO}
belonging to	PBMA				nitrophenyl groups			PBMA

The XPS survey spectrum (Figure 2a) of a 10 nm thick PBMA film got by SEEP displays two peaks at 83.8 and 87.5 eV, which can be easily attributed to the gold substrate. Indeed, as XPS is sensitive only to the outer 10−15 nm of the coating (mean escape depth of electrons in a polymeric material), with a very thin PBMA sample (≤10 nm), electrons of the substrate emerge and gold peaks (Au 4f 5/2 and Au 4f 7/2) are more or less visible on the survey spectrum. In Figure 2a, gold peaks are barely visible, indicating that the organic layer thickness is close to the sampling depth of the technique. Consequently, the whole thickness of the film, from the interface with gold to the upper part, was actually probed by XPS in the present case.

Figure 2a displays the characteristic carbon and oxygen peaks of PBMA[65] respectively centered at 285 and 532 eV. The O1s core level (Figure 2b) is composed of two peaks of same area attributed to the C−O and C═O groups in stoichiometry 1:1 in the PBMA. Regarding carbon signal, C1s core level spectrum (Figure 2c) presents three peaks. The smaller one at a higher binding energy (289 eV) corresponds to the carbonyl ester group COO, alkyl groups ($-CH_2-$, $-CH_3$) appear in the peak centered at 284.9 eV, and the small component at 286.5 eV was assigned to the ester −C−O− simple bond.

(65) Beamson, G.; Briggs, D. *High-Resolution XPS of Organic Polymer: The Scienta ESCA300 Database*; John Wiley & Sons: New York, 1992.

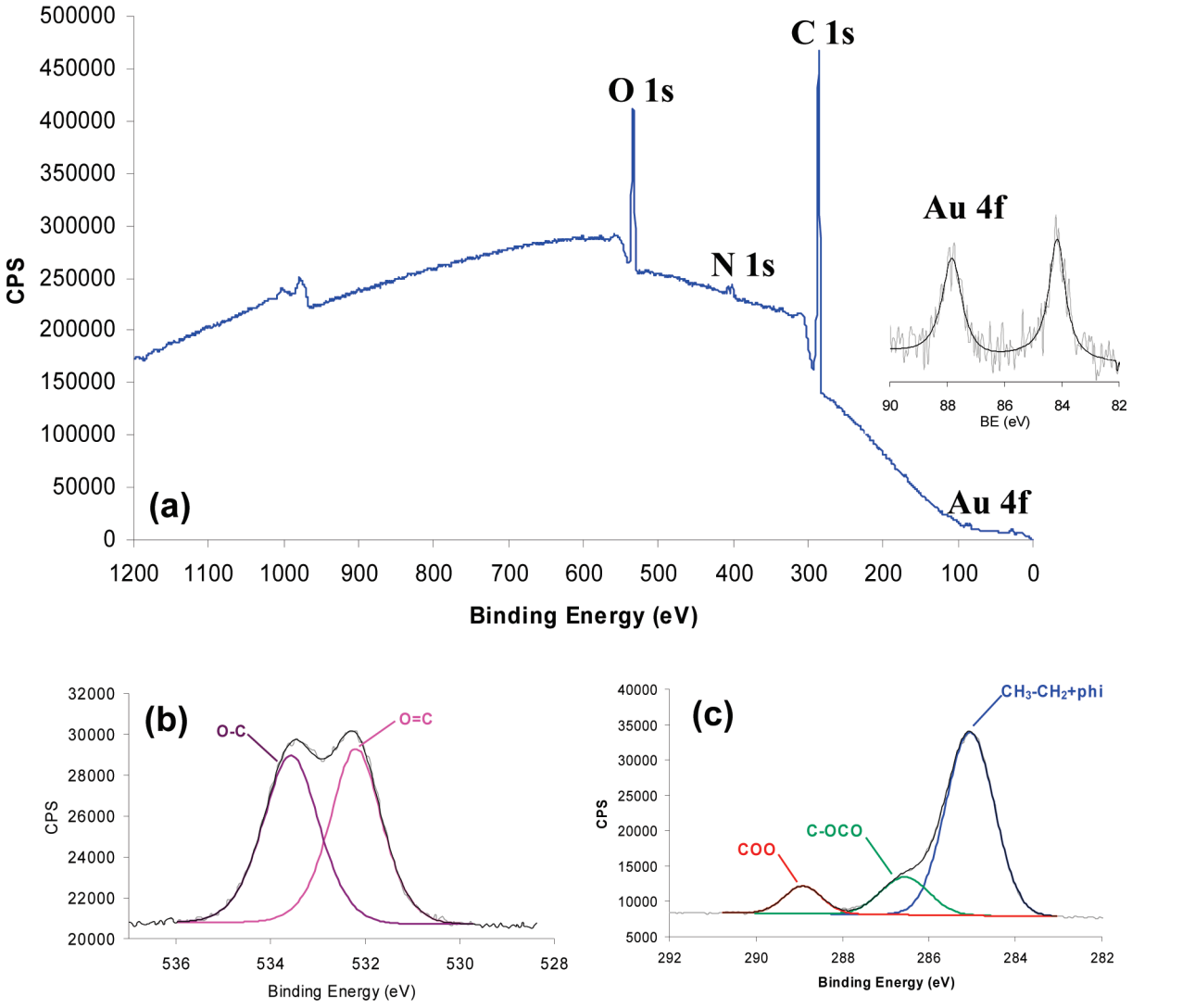

Figure 2. (a) XPS survey spectrum; (b) C1s core level spectrum; and (c) O1s core level spectrum of PBMA film (10 nm thick) grafted by SEEP of BMA in miniemulsion (5 cycles/−1.0 V/10 mV s^{-1}) on gold substrate.

The nitrogen area (around 400 eV) is detailed in Figure 3. The highest-energy peak at 406 eV was obviously attributed to the N1s in nitro groups ($-NO_2$). According to the literature, the first component at 399.3 eV can be attributed to amino groups ($-NH_2$) and the second one at 400.4 eV to azo groups ($-N{=}N-$). Those attributions will be discussed later in the section 3.4.

Hence, the reduction of BMA/NBD mixtures led to strongly grafted PBMA films that contained nitrophenyl groups, azophenyl groups, and aminophenyl groups, all coming from the reduction of NBD.

3.2. Film Structure Determination. To understand the mechanism of the SEEP process, it was essential to determine and establish a fine PBMA film structure. The main point of this task was to localize the nitrophenyl groups (Φ-NO_2) in the film. We already know that nitrophenyl radicals from NBD reduction form a polynitrophenylene-like layer according to the mechanism described in the literature[25,36,44,45] and that they are able to initiate radical polymerization.[56,57] Our previous work gave indications that a PNP-like "primer layer" was formed on the electrode, because the nitro signature was detected only with XPS on very thin films. So, the question is are nitrophenyl groups concentrated only at the gold interface in that PNP-like sublayer? Detailed analyses using IR-ATR, XPS, and ToF-SIMS will provide an answer.

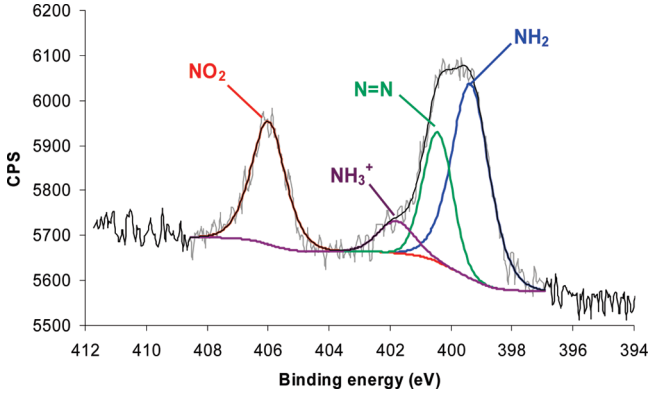

Figure 3. N1s core level XPS spectrum of PBMA film (10 nm thick) grafted by SEEP of BMA in miniemulsion (3 cycles/−1.0 V/10 mV s^{-1}) on gold substrate.

Table 2. Intensity of Mitrophenyl (Φ-NO_2) IR Absorption Bands in a PNP Film and in a PBMA Film Synthesized by SEEP

films	compds	ν_{NO2} band (1346 cm^{-1}) (%)	ν_{NO2} band (1522 cm^{-1}) (%)	$\nu_{C=C}$ band (1597 cm^{-1}) (%)
PNP	NBD	0.70	0.59	0.36
PBMA	SDS, BMA, NBD	2.21	1.59	1.05

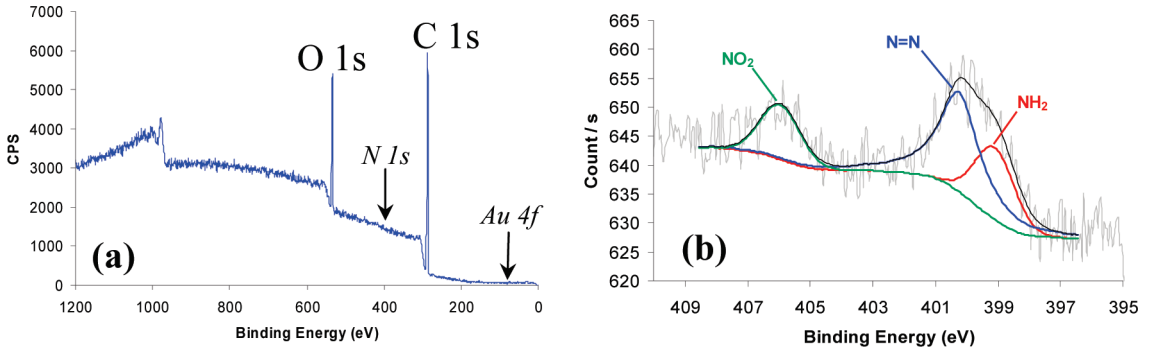

Figure 4. (a) XPS survey spectrum and (b) N1s core level spectrum of PBMA (50 nm thick) grafted by SEEP of BMA in miniemulsion (5 cycles/−1.0 V/10 mV s^{-1}) on gold substrate.

3.2.1. IR-ATR. Two samples were compared by IR-ATR (see the Supporting Information, Figure SI-2) with a focus on the intensity of the nitro group absorption bands, signature of nitrophenyl moieties. The first sample was a PNP-like layer made by electrochemistry (5 cycles, −1.0 V, 10 mV/s) from an acidic solution (1×10^{-2} M) of NBD (0.0237 g, 2×10^{-3} mol.L^{-1}) alone without monomer. The second one was a PBMA film made by SEEP as described in the Experimental section (acidic miniemulsion containing NBD and BMA) under the same electrochemical conditions. The aryldiazonium concentration was the same in both cases (2×10^{-3} M). Besides the apparition of the PBMA carbonyl band at 1730 cm^{-1} in the second case, the main differences are the intensity values (Table 2) of the three nitrophenyl group characteristic bands, which are three times higher when BMA monomer is present (second case). Two explanations can be proposed to elucidate that increase of the nitrophenyl amount in the film. (i) The PNP sublayer was three times thicker in presence of BMA; (ii) nitrophenyl moieties were not located in the PNP sublayer only. The former rationale was unlikely since NBD electroreduction and PNP grafting should not be significantly influenced by any neutral species present in the solution. Therefore, the most likely hypothesis was that nitrophenyl groups were incorporated into the PBMA chains throughout the entire film.

3.2.2. XPS Analysis. As seen in the first part, for thin PBMA samples where gold peaks are visible on the survey spectrum, N1s signals are detected. On the contrary, for samples whose thickness is significantly higher than the analysis depth (more than 15 nm), gold peaks are not visible anymore from the survey spectrum, as seen in Figure 4a. In that case, N1s peaks originating only from a PNP sublayer located directly at the gold interface should also be absent from the spectrum. However, an N1s signal is still present (Figure 4b), which means that nitrophenyl groups are not only present at the gold−film interface as a sublayer but are also present throughout the entire PBMA film.

3.2.3. ToF-SIMS profile. ToF-SIMS profile allows a detailed analysis of the whole thickness of the film, from the upper (superficial) part to inner part (interface area). Indeed, the coating profile (Figure 5) gives the normalized intensity of the collected ionized fragments resulting from ion bombardment of the PBMA grafted film versus digging time (which is directly related to the film thickness). Time zero corresponds to the top of the film and at the final time, the substrate is reached. For the sake of clarity, only one fragment profile from nitrophenyl moieties (CNO; m/z = 42.0, green line) and two from PBMA (C_2H, m/z = 25.01; C_4H_5O, m/z = 85.04, purple lines) are represented. The gray line is the gold substrate profile. PBMA fragments (purple curves), keep a high intensity (70 − 90%) during almost all the digging time (≡ film thickness) and start to decrease only when the gold signal is reached. This is consistent with the chemical composition of the grafted films, which is almost pure PBMA. On the contrary, nitrophenyl fragments (CNO, green line) increase when reaching the substrate, with a slope almost similar to the gold one (gray line), which is consistent with the presence of a very thin PNP sublayer, whose thickness is related to the shift in digging time between the green and gray lines. However, nitrophenyl fragments are also extracted from the top part of the film: indeed, the intensity recorded at low digging times is far from negligible. If nitrophenyl moieties were only located in a sublayer, the green signal should be zero at low digging time and should increase progressively in parallel to the gold one. The significant signal observed at low digging time (top part of the film) undoubtedly demonstrates that nitrophenyl moieties are present throughout the entire film. Therefore, nitrophenyl groups/CNO profile is in perfect agreement with the previous analyses: nitrophenyl groups are located in high concentration close to the substrate, forming a PNP sublayer at the interface with gold and they are also spread in lower concentration throughout the full polymer thickness up to the top of the film.

In conclusion of this part, our three analyses converge on the same film structure. Starting from the substrate, a pure PNP-like (= $(\Phi\text{-}NO_2)_n$) thin grafted layer, resulting

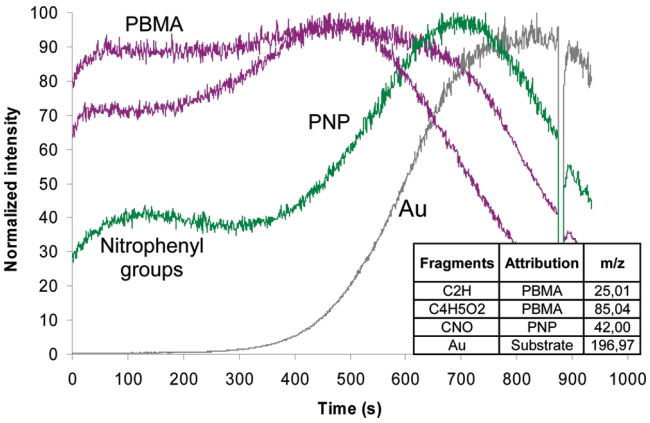

Figure 5. ToF-SIMS profile of PBMA film grafted by SEEP of BMA in miniemulsion (5 cycles/−1.0 V/10 mV s^{-1}): $C_xH_y(O_z)$ fragments (red) from PBMA, CNO fragments (green) from nitrophenyl groups, Au profile (gray). Insert table gives fragments attribution according to m/z ratio.

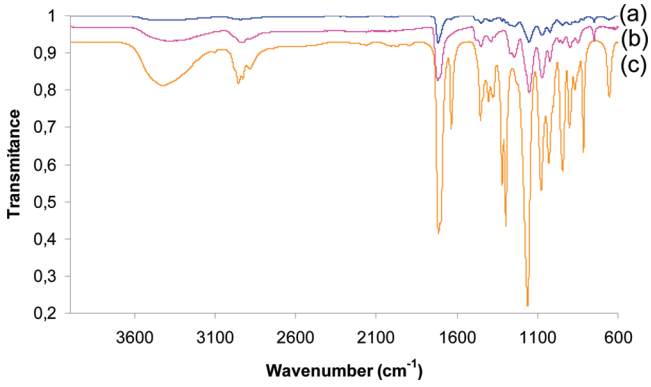

Figure 6. IR-ATR spectra of (a) PHEMA collected after 15 h of chronoamperometry (−1.0 V) from HEMA in acidic medium; (b) Commercial PHEMA (20 000 g mol^{-1}); and (c) commercial HEMA monomer.

directly from NBD reduction. Then, PBMA chains attached to the PNP sublayer are found with nitrophenyl groups dispersed regularly in the PBMA part.

The structure of the grafted films provided by SEEP is thus well established. However, in order to propose a full mechanism for their formation, we still need to understand which reactions are involved.

3.3. Proton Reduction and Role of Hydrogen Radicals. Experiments results are reported here to highlight the role of hydrogen radical as a polymerization initiator.

3.3.1. Without Diazonium Salts. In our previous article, we already demonstrated that without NBD in the starting medium, no polymer was found grafted on the electrode as suggested by IR spectrum (see the Supporting Information, Figure SI-3), but polymer chains were found in solution. This former experiment strongly suggested that (i) radical species issued from the electroreduction of protons are able to initiate the radical polymerization of the vinylic monomers in solution; (ii) the PNP primer layer is essential to graft the vinylic polymer onto the substrate. This result assumes that alkyl macroradicals (from propagation) are less reactive than aryl radicals (from nitrobenzene diazonium reduction) toward gold surfaces.

A new experiment was carried out to reinforce those hypotheses in which a hydrosoluble monomer, hydroxyethyl methacrylate (1.0 mol L^{-1} water solubility), was used instead of BMA to avoid any demixtion of the miniemulsion during the long-time reaction. HEMA (6.53 g, 1.0 mol L^{-1}) was poured in 50 mL of acidic water (H_2SO_4−DI H_2O, 1×10^{-2} mol L^{-1}) and submitted to chronoamperometry at −1.0 V for 15 h. The recorded current decreased from 10 to 3 mA, likely because of physisorbed matter. At the end, the reaction mixture was separated, and water was evaporated under a vacuum. The oily residue was then dried under a vacuum for 30 h. Finally, 5.193 g of a white solid was collected (80% conversion). IR spectrum clearly exhibits characteristic bands of PHEMA with no residue of HEMA (Figure 6). Hence, HEMA did polymerize, although it could not be directly reduced at the cathode in those conditions, because its redox potential (≈ −2.5 V) was never reached. In the absence of diazonium salt, hydrogen radicals ($H^{\bullet}$) generated from protons reduction are the only species able to initiate a radical polymerization in the above conditions. As we already saw that similar currents are also observed in SEEP conditions in the same potential window, it is likely hydrogen radicals are also generated in SEEP when the potential reaches −0.5 V and eventually play a role in initiating the vinylic polymerization, together with aryl radicals issued from the reduction of NBD.

3.3.2. Variation of Final Potential. Figure 7a gives the measured thickness recorded on grafted PBMA films with profilometry together with the transmittance intensity recorded on the carbonyl absorption band in the IR spectrum for various final potential values. There is obviously a direct relationship between the final thickness of the grafted film and the potential window experienced by the reacting medium: the more cathodic the final potential, the thicker the grafted film. As the amount of reduced protons also increases when the potential becomes more cathodic, Figure 7a confirms that hydrogen radicals resulting from protons reduction play an important role. Moreover, Figure 7b shows that when the final potential of the cyclic voltamperometry is stopped before proton reduction regime (i.e., above c.a. −0.4 V vs SCE), the grafted film is thinner than when protons are reduced.

3.3.3. EQCM Experiment. EQCM allows simultaneous measurement of electrochemical parameters (i.e., current, charge, etc.) and mass changes at electrode surfaces via changes in the resonant frequency of the quartz crystal. Thus, decreases in mass correspond to increases in frequency and vice versa. Considering that the deposited layer is rigid and that no viscoelastic changes occur at the electrode interface, the frequency and mass changes are related by a simple, linear equation: $\Delta f = -C_f \Delta m$ (Sauerbrey equation) where Δf (Hz) is the frequency change, Δm (μg cm^{-2}) is the mass change, and C_f (Hz cm^2 μg^{-1}) is the proportionality characteristic constant of the 9 MHz quartz crystal used (including the shear modulus, the quartz density and the piezoelectric active area).

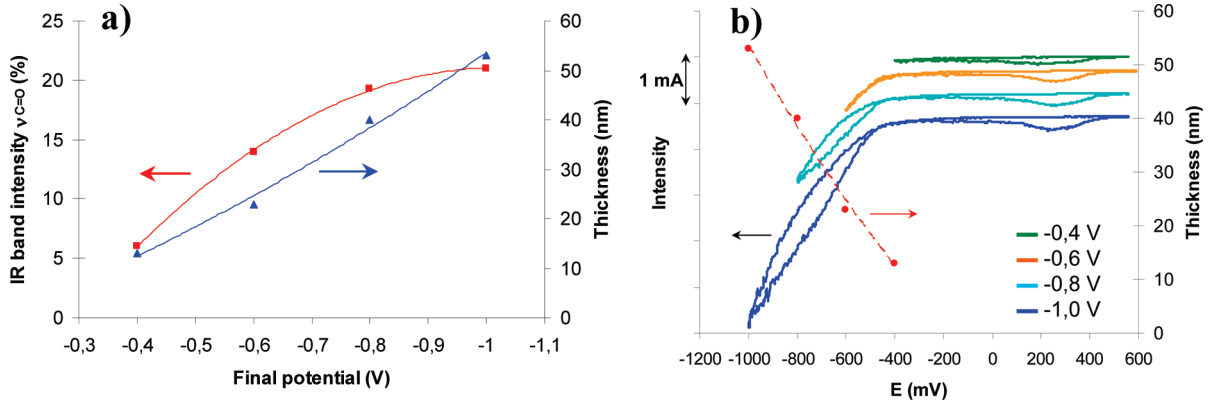

Figure 7. (a) IR $\nu_{C=O}$ band transmittance intensity (red) and profilometer-measured thickness (blue) of PBMA films grafted by SEEP of BMA in miniemulsion (5 cycles/10 mV s^{-1}) versus final potential. (b) Thicknesses versus final potential of PBMA films grafted by SEEP of BMA in miniemulsion (5 cycles/10 mV s^{-1}) (red) superimposed to the corresponding 1st cycle of voltamperogramm ($I = f(E)$) recorded (for clarity sake, only the first cycle of the voltamperogramm has been represented).

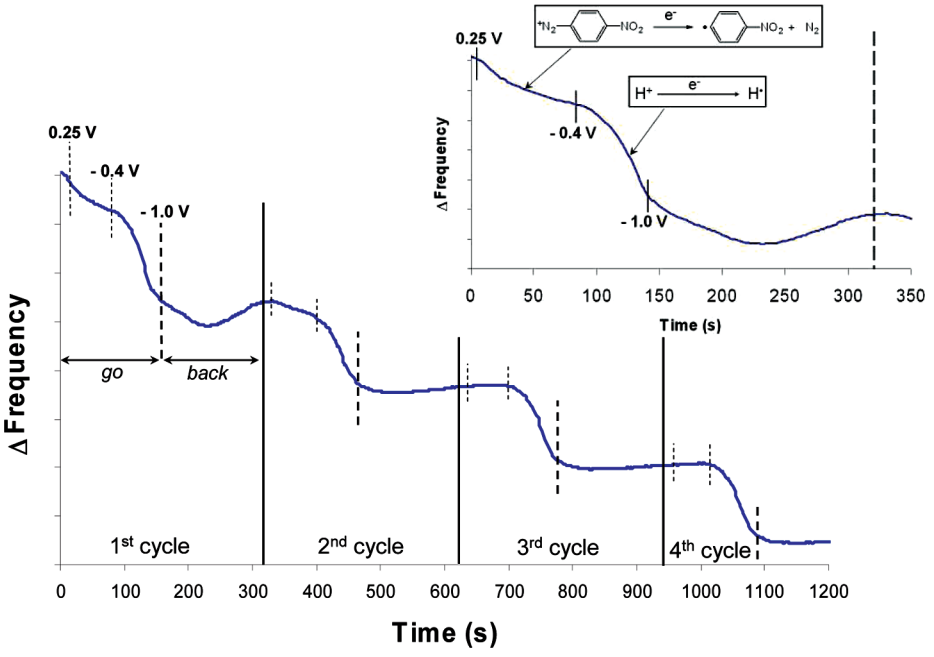

Figure 8. Quartz frequency variation versus time for successive voltamperometric cycles in SEEP of BMA in miniemulsion (4 cycles/−1.0 V/10 mV s^{-1}) on gold substrate. Insert: zoom of the 1st cycle.

Quartz was connected as working electrode and cyclic voltamperometry (4 cycles/−1.0 V/10 mV s^{-1}) was performed as usual. The frequency change versus time is reported in Figure 8 and split according to the four electrochemical cycles. If we focus on the first one (from 0 to 315 s, see insert Figure 8), two regions can clearly be distinguished: (i) from 0.25 to −0.4 V, the first mass increase can be attributed to the diazonium reduction; (ii) and then from −0.4 to −1.0 V, an important mass variation occurs within the proton reduction regime, which almost stops at −1.0 V. At the end of the first cycle, a small amount of nongrafted matter is desorbed. In the second cycle, the diazonium reduction effect is still visible but less important than on the first cycle and from the third cycle to the end, there is no more observable frequency change between 0.25 V and −0.4 V. In the same time, frequency decrease still occurs in the proton reduction regime with the same intensity at each cycle. This EQCM result means that during proton reduction there is an important mass increase at each cycle, even when diazonium reduction is almost negligible. Thus, hydrogen radicals play an important role in the building process at each voltamperometric cycle, whereas the effect of nitrophenyl radicals from diazonium cation reduction on the film formation is only significant on the first two cycles. This is consistent with the increasing difficulty for diazonium cations to reach the gold surface when the film thickness increases, while protons still find their way.

3.3.4. Grafting in Two Steps. SEEP is a one-pot process, meaning that all reactions occur simultaneously in the reactor. For a better understanding, the grafting was then decomposed in two separated steps: (i) first, electrografting of a PNP-like film by reducing NBD alone from an aryldiazonium acidic solution; (ii) using this PNP-modified gold substrate as a working electrode in SEEP medium without NBD. On the IR-ATR results

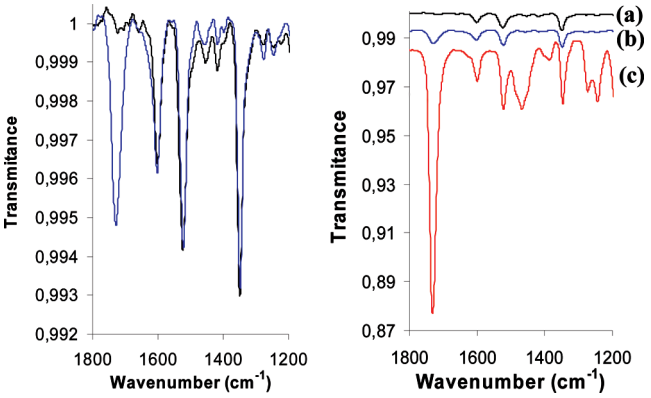

Figure 9. (Left) IR-ATR spectra of PNP sublayer after the first step (black) and PBMA after the second step (blue). (Right) IR-ATR spectra comparison of (a) PNP after the first step; (b) PBMA after the second step (5 cycles/−1.0 V/10 mV s^{-1}); and (c) PBMA grafted by one-pot SEEP (5 cycles/−1.0 V/10 mV s^{-1}).

Table 3. Intensity of the Carbonyl IR Band in PBMA Film Synthesized in Two Steps or after a Classical SEEP in One Step

	two-step experiment	one-step experiment
$\nu_{C=O}$ intensity (%)	0.5	10−15

(Figure 9), the characteristic band of the PBMA carbonyl group at 1730 cm^{-1} highlights that PBMA is formed and grafted on the PNP sublayer. Furthermore, from the first to second step, XPS signals of C1s and O1s core levels were modified from PNP to PBMA characteristic signals (see the Supporting Information, Figure SI-4) confirming PBMA grafting. However, despite the same concentrations being used in both cases, the carbonyl IR band intensity was 10 times weaker when the grafting was performed in two steps than in "classical" one step (Table 3), suggesting that PBMA grafting was clearly less efficient in two steps (Figure 9). An explanation of this phenomenon is developed in the next part.

Knowing that no aryldiazonium initiators were present in solution in the second step, this latter experiment strongly suggests that PBMA grafted chains were initiated by hydrogen radicals from protons reduction. However, another likely hypothesis could be that PNP sublayer was damaged when crossed by a cathodic current (∼10 mA) in the second step and released some nitrophenyl radicals entities able to initiate the polymerization of BMA. To discard that hypothesis, we also performed the second step under chemical activation instead of electrochemical reduction.[66] In this case, a chemical reducer (iron powder) was added in the medium to replace the cathodic current. Indeed, the Fe/Fe^{2+} couple, the redox potential of which is −0.44 V vs NHE (−0.69 V vs SCE), is able to reduce protons. A PNP-modified gold substrate was dipped for 1 h in a solution containing HCl 0.5 M (52 mL), HEMA (2 mL), and iron powder (1.899 g). After being rinsed in DI H_2O under ultrasound (power 50%) for 5 min, the sample was characterized by IR (see the Supporting Information, Figure SI-5), contact angle measurement (Table 4), and XPS (see the Supporting Information, Figure SI-6). The IR spectrum exhibits a characteristic major absorption band at 1729 cm^{-1} related to the PHEMA carbonyl group. The decreasing contact angle from 86° for the PNP to 57° after the second step confirms that a hydrophilic layer of PHEMA was grafted. Lastly, C1s and O1s XPS signals are typically those of a PHEMA film. Analyses clearly indicate that PHEMA was grafted in the second step attesting that HEMA radical polymerization was indeed initiated by hydrogen radicals and not by nitrophenyl radicals resulting from damage electrochemically induced in the PNP sublayer.

(66) Mévellec, V.; Roussel, S.; Tessier, L.; Chancolon, J.; Mayne L'Hermite, M.; Deniau, G.; Viel, P.; Palacin, S. *Chem. Mater.* **2007**, *19*, 6323–6330.

Table 4. Contact Angle Measured on PNP Sublayer after the First Step and on PHEMA Film Grafted in the Second Step Using a Chemical Reducer (Iron Powder)

	first step	second step
	PNP	PHEMA
contact angle (deg)	86.62 ± 2.91	56.84 ± 4.39

3.4. Proposed Mechanism of SEEP. From all analyses and experimental results detailed above, it was possible to elaborate a SEEP mechanism including classical radical polymerization steps, namely, initiation, propagation, and termination. If initiation and propagation are quite similar to those in a bulk radical polymerization, termination reaction leads, in SEEP, to the polymer grafting. As usual, initiation involves two reactions; first, primary radical generation by electrochemical reduction and then initiation by reaction with a vinylic monomer. Termination corresponds to the "grafting to" step of PBMA chains on the substrate. Moreover, SEEP mechanism includes an additional reaction at the beginning, which is the PNP-like layer formation. Now let us describe a more plausible mechanism, split in the three classical polymerization steps.

3.4.1. Initiation. The initiation step starts when radicals are generated by electrochemical reduction in the vicinity of the polarized electrode. Nitrobenzene diazonium cations and protons are respectively reduced in nitrophenyl radicals ($^{\bullet}\Phi$-NO_2) and hydrogen radicals ($H^{\bullet}$) by a cathodic current:

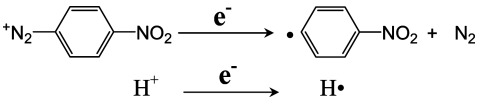

One of the key points of the mechanism is that aryl radicals generated by the electroreduction of NBD play a double role. (1) On the one hand, they form a primer polynitrophenylene-like grafted layer on the cathode[20] (see the Supporting Information, Scheme SI-1). However, if the formation of this PNP layer is incontestable with a mechanism widely reported in the literature,[44,45] our XPS results (Figures 3 and 4b) show azo linkages (-N=N-) and amino groups ($-NH_2$) leading to quite a complex structure (see the Supporting Information, Scheme SI-2). The literature confirms the presence of azo and amino groups in such films, but the mechanism of their formation is still

Scheme 2. Chemical Mechanism of (top) Nitrophenyl Radical and (bottom) Hydrogen Radical Initiation and Propagation Steps of Radical Polymerization

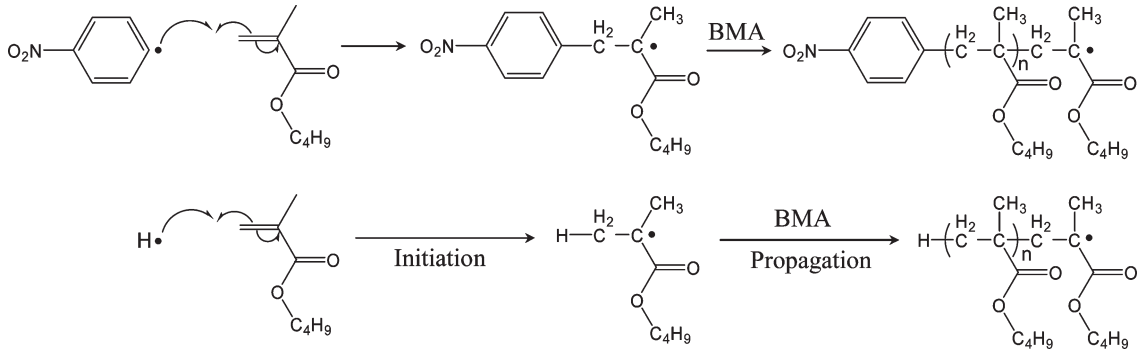

under debate.[67] For the azo linkages, one hypothesis is to suggest an azo coupling reaction between diazonium cation and an electron-rich aromatic ring;[31,68] a second one proposes an alternate electroreduction pathway of the diazonium group leading to a diazenyl radical;[30] and a third tentative mechanism, recently offered by Pinson et al., suggests the attack of the diazonium cation on a cyclohexadienyl radical.[69] Regarding amino groups, they were for a long time explained by the electrochemical reduction of nitro groups in an acidic medium,[70−74] but a second hypothesis implies chemical reduction of NO_2 under the X-ray beam during XPS experiment.[4,34,75] (2) On the other hand, as recently reviewed and observed in our experiments, aryl radicals ($^{\bullet}\Phi$-NO_2) are very good radical sources to initiate radical polymerization.[56,57] Moreover, many results shown in the previous part indicate the importance of the proton reduction (QCM and two-step experiment). Even when diazonium salt is missing, polymer is detected in bulk, proving that hydrogen radicals ($H^{\bullet}$) are able to initiate radical polymerization too in our conditions. Indeed, although the major product of proton reduction is dihydrogen, hydrogen radical intermediates have been shown to act as radical polymerization initiators.[76−78] Tashiro et al.[79] already reported that the mechanism of an electrochemically induced polymerization reaction is assumed to be initiated by the attack of electrochemically generated hydrogen radicals onto 4-vinylpyridine monomers. More recently, Cram et al.[80] described a mechanism of electropolymerization of methyl methacrylate on stainless steel in sulphuric acid, which also involved hydrogen radicals. We assume a similar process occurs in SEEP: there is a double initiation $^{\bullet}\Phi$-NO_2/$H^{\bullet}$ and oligo-radical chains in growth thus possess two different extremities according to their initiator, either $O_2N-\Phi-$-CH_2- or $H-CH_2-$ (Scheme 2). An obvious consequence of the above conclusion is that initiation very likely occurs in the water phase within the biphasic system. Indeed, as NBD salts are more soluble in water than in BMA and protons are localized in water, initiation is likely to occur in the continuous aqueous phase with the small amount of BMA soluble in water (water solubility of BMA at saturation = 2.5×10^{-3} mol/L at 25 °C).[81]

3.4.2. Propagation. BMA is essentially consumed by propagation in the aqueous solution (very probably in the vicinity of the electrode surface), which is then continuously supplied via monomer diffusion from the droplets (similarly to what happens in a conventional emulsion polymerization, with monomer diffusion from the droplets to the particles through the aqueous phase).[81,82] For a hydrophobic polymer such as PBMA, the formed oligoradicals reach a critical polymerization degree, $DP_{n,crit}$, beyond which they cannot stay in the aqueous phase. They will then diffuse toward the hydrophobic phase of the medium. The latter can be the surfactant micelles, if any (after ultrasonication, SDS is usually adsorbed on the water/droplet interface below the saturation threshold, which prevents micelles from forming[83]), the monomer droplets or the organic interfacial film grafted to the gold electrode. Because of very small overall monomer conversion (4−5%), and the absence of polymer particles in the polymerization medium, diffusion of the oligoradicals toward micelles or droplets seems to be negligible. It is then assumed that most of them will be trapped in the polymer layer at the electrode surface,

(67) Combellas, C.; Delamar, M.; Kanoufi, F.; Pinson, J.; Podvorica, F. I. *Chem. Mater.* **2005**, *17*, 3968–3975.
(68) Toupin, M.; Belanger, D. *J. Phys. Chem. C* **2007**, *111*, 5394–5401.
(69) Doppelt, P.; Hallais, G.; Pinson, J.; Podvorica, F.; Verneyre, S. *Chem. Mater.* **2007**, *19*, 4570–4575.
(70) Baizer, M. M. *Organic Electrochemistry*; Marcel Dekker: New York, 1973.
(71) Delamar, M.; Désarmot, G.; Fagebaume, O.; Hitmi, R.; Pinson, J.; Savéant, J.-M. *Carbon* **1997**, *35*, 801–807.
(72) Saby, C.; Ortiz, B.; Champagne, G. Y.; Belanger, D. *Langmuir* **1997**, *13*, 6805–6813.
(73) Brooksby, P. A.; Downard, A. J. *Langmuir* **2004**, *20*, 5038–5045.
(74) Actis, P.; Caulliez, G.; Shul, G.; Opallo, M.; Mermoux, M.; Marcus, B.; Boukherroub, R.; Szunerits, S. *Langmuir* **2008**, *24*, 6327–6333.
(75) Mendes, P.; Belloni, M.; Ashworth, M.; Hardy, C.; Nikitin, K.; Fitzmaurice, D.; Critchley, K.; Evans, S.; Preece, J. *ChemPhysChem* **2003**, *4*, 884–889.
(76) Teng, F. S.; Mahalingam, R.; Subramanian, R. V.; Raff, R. A. V. *J. Electrochem. Soc.* **1977**, *124*, 995.
(77) Teng, F. S.; Mahalingam, R. *J. Appl. Polym. Sci.* **1979**, *23*, 101–113.
(78) MacCallum, J. R.; MacKerron, D. H. *Eur. Polym. J.* **1982**, *18*, 717–724.
(79) Tashiro, K.; Matsushima, K.; Kobayashi, M. *J. Phys. Chem.* **1990**, *94*, 3197–3204.
(80) Cram, S. L.; Spinks, G. M.; Wallace, G. G.; Brown, H. R. *Electrochim. Acta* **2002**, *47*, 1935–1948.
(81) Gilbert, R. G. *Emulsion Polymerization, A Mechanistic Approach*; Academic Press: London, 1995.
(82) Lovell, P. A.; El-Aasser, M. S. *Emulsion Polymerization and Emulsion Polymers*; John Wiley & Sons: Chichester, U.K., 1997.
(83) Landfester, K. *Macromol. Rapid Commun.* **2001**, *22*, 896–936.

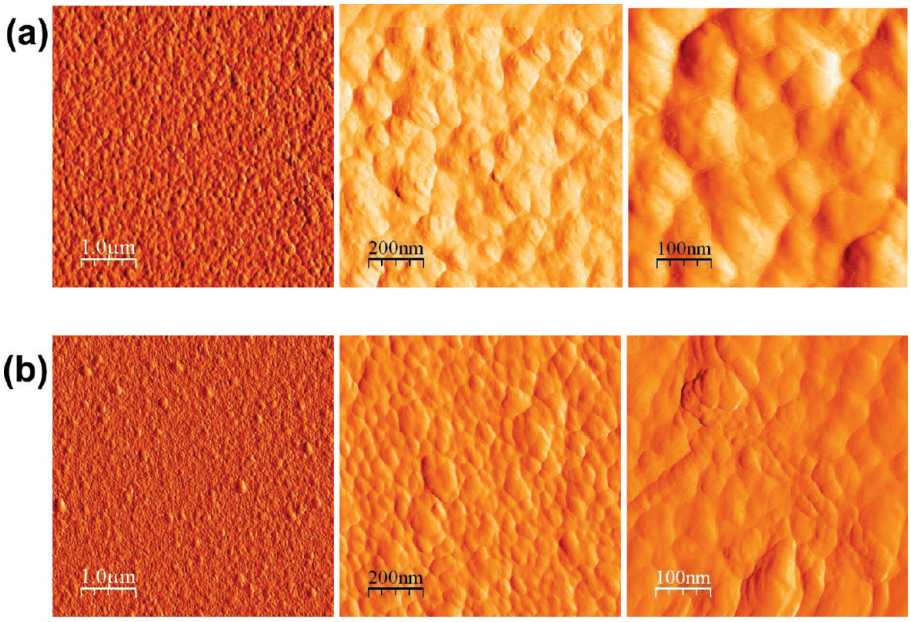

Figure 10. AFM pictures in tapping mode of (a) PBMA films and (b) PHEMA films grafted by SEEP on gold substrate, at different scales (5×5, 1×1, and 0.5×0.5 μm^2).

where grafting will further take place, via termination or chain transfer reactions, as detailed in the next section. Because of the presence of a noncharged initiator fragment at the chain-end (see Scheme 2), the $DP_{n,crit}$ value should be very small (a few units). Actually, PBMA chain length was roughly estimated by calculating an approximate polymerization degree from XPS results. In this calculation, we made the approximation that each polymer chain is initiated by a nitrophenyl radical and therefore, all the chains bear a nitrophenyl end containing a nitrogen atom. Hence, the polymerization degree is calculated from the C/N ratio given by XPS results. The number of monomer units incorporated in the grafted chains calculated from this approximation, is about 10−12. In contrast, for a polymer with higher water solubility such as PHEMA, $DP_{n,crit}$ should be higher and films tend to be thicker. This assumption is confirmed by our results: all conditions being equal (5 cycles/−1.0 V/10 mV s^{-1}/0.7 mol L^{-1}), the PHEMA film is 70 nm thick, whereas the thickness of PBMA film is 20 nm. Furthermore, PBMA films morphology was probed by AFM. PBMA film pictures recorded at different scales clearly evidenced a globular morphology which is probably due to the poor affinity between the solvent (water) and the polymer chains. As water is a bad solvent for PBMA, chains tend to aggregate, giving rise to "mushrooms" structure (Figure 10a). On the contrary, grafted films prepared from a water-soluble monomer (HEMA) look smoother and more homogeneous (Figure 10b).

3.4.3. Chain Transfer/Termination at the Electrode Surface. Once they adsorb onto the PNP-like layer at the electrode surface, the oligoradicals can undergo chain transfer or termination reactions, which will stop their growth. In radical polymerization, it has been shown that the presence of aromatic nitro compounds such as nitrobenzene leads to transfer reactions.[84] In a similar way, in SEEP, radical extremity of oligoradicals may attack aromatic rings of nitrophenyl moieties from the PNP layer by an addition−elimination reaction (Scheme 3). As radical aromatic substitution is not very sensitive to substituent directive effects, PBMA chains can add indifferently on any positions versus NO_2 on the aromatic ring. However, because of the steric hindrance due to the aryl−aryl bond in para position versus NO_2, the more likely position to link PBMA chains may be the ortho position versus NO_2, which is more accessible than the meta position.

When aromatic ring sites of the PNP are no longer available, the film growth is not yet stopped. Indeed, some grafted chains present a nitrophenyl extremity, according to their initiation, leaving new "hosting sites" for macroradical chains to terminate and film thickness grows up by successive termination of propagating PBMA chains on nitrophenyl sites (Scheme 4a). Obviously, film thickness (i.e., IR transmittance intensity of $\nu_{C=O}$ band) depends on the number of voltamperometric cycles (see the Supporting Information, Figure SI-7). Consequently, the grafted PBMA chains, which present a proton end, should tend to limit the film thickening. This is consistent with our results in the two-step experiment where the only initiators in the vinylic polymerization were hydrogen radicals leading to CH_3 extremities only, inefficient for film thickening (Scheme 4b). The final thickness was found to be 10 times smaller than in classical SEEP conditions (Table 3). Hence, nitrophenyl moieties act like nodes or cross-linkers between PBMA chains, which is in good agreement with the structure determined before.

4. Conclusion

The new SEEP technique presents several advantages: experiments are performed in water, in a one-pot process,

(84) Odian, G. *Principles of Polymerization*; JohnWiley & Sons: New York, 2004

Scheme 3. Chemical Mechanism of PBMA Chains Linkage on the Polyaryl Sublayer by an Addition−Elimination on the Aromatic Ring

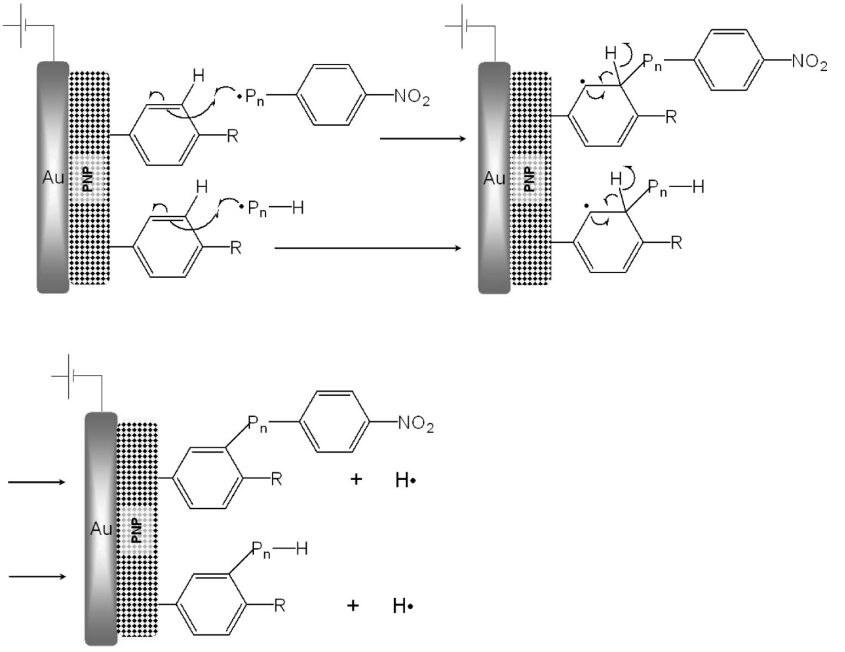

Scheme 4. (a) Structure of PBMA Films by SEEP; Polymer Chains Have Two Different Ends (either CH_3 or Φ-NO_2) According to Their Initiator; (b) Structure of PBMA Films Synthesized in the Two-Step Experiment; Polymer Chains Have Only CH_3 Ends, Which Gives Thinner Grafted Films

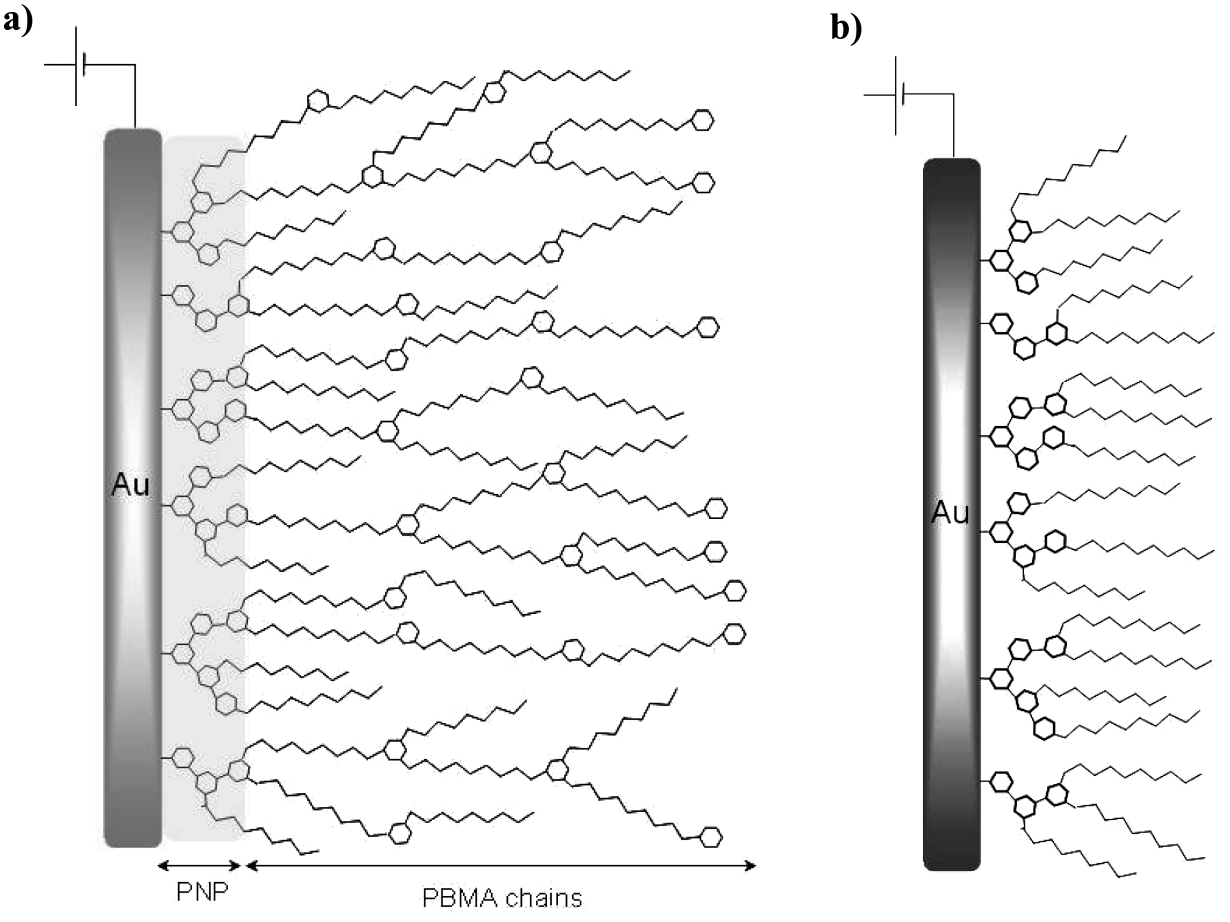

on any conducting or semiconducting substrates, in one fast electrochemical step, at room temperature. The method relies on the ability of diazonium salts to be easily electrografted on conducting surfaces under moderate cathodic conditions and act both as initiator for the conventional radical polymerization of vinylic monomers

and as primer sublayer. The novelty of this new "grafting to" process is based on the originality of the mechanism, with which it seems easy to achieve multilayered polymer films (i.e., in several consecutive steps with different monomer emulsions) or statistic copolymer films (in one step by mixing both monomers together in the same reaction medium). The mechanism can be split in three steps:

Electrochemical initiation giving rise to protons and diazonium cations reduction.

Radical initiation by nitrophenyl and hydrogen radicals and simultaneously formation of the PNP sublayer, followed by propagation.

Chain transfer/termination of PBMA oligoradicals on the aromatic rings of the PNP sublayer.

More results, not presented here, indicate that the SEEP process can be applied to any conducting substrate, with any monomer able to polymerize through a radical mechanism (mainly methacrylates and acrylates). On the other side, additional works are in progress to understand more precisely the role of the surfactant nature (anionic, neutral, or cationic) and the donor or acceptor nature of the substituting group on the aryldiazonium salt ($-O-CH_3$ or $-NO_2$).

More generally, SEEP has been successfully used for applications such as hydrophobic/hydrophilic patterning of gold surface and carbon nanotubes functionalization.[60]

Acknowledgment. The authors thank Alchimer S.A. and more particularly Sylvie Verneyre for ToF-SIMS profiles; Pascale Jégou and Nabila Debou for XPS analyses and Federico Grisotto for AFM pictures from CEA, SPCSI laboratory.

Supporting Information Available: Additional information (PDF). This material is available free of charge via the Internet at http://pubs.acs.org.